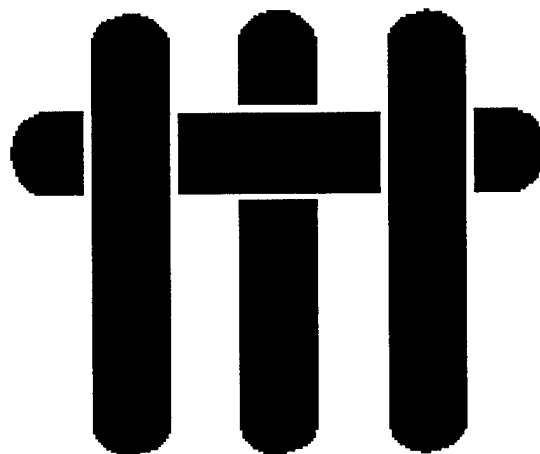


M A T E R I A L S



Reliable Ceramic Structural Composites Designed with a Threshold Strength

Technical Report # 4

Factors Affecting Threshold Strength in Laminar Ceramics with Thin Compressive Layers

M. P. Rao and F. F. Lange

Period: 5/00 through 4/30/01

Office of Naval Research

Grant No. N00014-99-1-0638

Fred F. Lange, Principal Investigator

Materials Department
University of California
Santa Barbara, CA 93106

DISTRIBUTION STATEMENT A

Approved for Public Release
Distribution Unlimited

20010227 093

Factors Affecting Threshold Strength in Laminar Ceramics with Thin Compressive Layers

M. P. Rao and F. F. Lange

Materials Department
University of California, Santa Barbara, CA 93106

Abstract

Compressive layers, placed within a laminate, can arrest cracks. With an increasing applied stress, the arrested crack can propagate through the compressive layer. These phenomena produce a material with a threshold strength, i.e., failure can not occur below a critical stress. A previously reported stress intensity function describes different variables, e.g., magnitude of compressive stress, thickness of compressive layer, distance between compressive layers, that govern the threshold strength. Laminar composites composed of thicker alumina layers separated by thinner alumina/mullite layers were fabricated to test the different variables that were predicted to govern the threshold strength. It is shown that the data agree well with the predicted values only when the magnitude of the compressive stress and/or the thickness of the compressive stress were low. For these conditions, the crack extended straight through the compressive layers as assumed by the model used to predict the threshold strength. On the other hand, when the compressive stress and/or the layer thickness were large the threshold strength was larger than the predicted value. In addition, for these conditions the crack bifurcated through the compressive layer. The angle between the bifurcated cracks increased with increasing compressive stress.

Introduction

It has been demonstrated [1] that uniformly spaced compressive layers can stop the otherwise catastrophic propagation of cracks, therefore truncating the statistical strength distribution of brittle materials to prevent failure at stress values below a specific stress. A stress intensity function was introduced [1] to describe how the arrested crack within the tensile layer is shielded from the applied stress as the crack propagates through the bounding layers containing biaxial, compressive stresses

$$K = \sigma_a \sqrt{\pi a} + \sigma_c \sqrt{\pi a} \left[\left(1 + \frac{t_1}{t_2} \right) \frac{2}{\pi} \sin^{-1} \left(\frac{t_2}{2a} \right) - 1 \right] \quad (1)$$

where σ_a is the applied tensile stress, a the half crack length, and t_1 and t_2 the thickness of the compressive and tensile layers, respectively. The magnitude of the biaxial, residual stress within the thinner, compressive layers, σ_c , can be described by [2]

$$\sigma_c = \varepsilon_r E_1 \left(1 + \frac{t_1 E_1}{t_2 E_2} \right)^{-1}$$

1

(2)

where ϵ_r is the residual differential thermal strain, $E_i' = E_i / (1 - \nu_i)$, E the Young's modulus, and ν_i the Poisson's ratio. Although Eq. (1) describes a new toughening phenomena, it was shown that after its rearrangement, a more profound statement could be made concerning the strength statistics of a brittle material [1]. Namely, it was shown that failure would only occur at a stress that would cause the crack to fully extended across the compressive layer. Using this obvious statement by setting $2a = t_2 + 2t_1$ and $K = K_c$, the critical stress intensity factor for the compressive layer material, Eq. (1) can be rearranged to produce an expression for a threshold strength, i.e., a stress below which failure cannot occur:

$$\sigma_{thr} = \frac{K_c}{\sqrt{\pi \frac{t_2}{2} \left(1 + \frac{2t_1}{t_2}\right)}} + \sigma_c \left[1 - \left(1 + \frac{t_1}{t_2}\right) \frac{2}{\pi} \sin^{-1} \left(\frac{1}{1 + \frac{2t_1}{t_2}} \right) \right] \quad (3)$$

The purpose of the current work was to experimentally determine the effect of the different independent variables in Eq. (3). This was accomplished through the fabrication and testing of an extensive series of different laminate architectures to determine the effect of three variables: the magnitude of residual compression, the thickness of the compressive layers, and the thickness of the thicker, tensile layers. As shown below, the model correctly predicts the threshold strength only when the compressive stress and/or the thickness of the compressive layer is small. For these cases, the crack propagates through the compressive layer as a single crack with increasing applied stress, as assumed by the model used to develop Eq. (3). On the other hand, when the compressive stress and/or the thickness of the compressive layer is large, the crack bifurcates within the compressive layer and produces a threshold strength much larger than predicted by Eq (3).

1 Experimental Procedure

2.1 Specimen Preparation

To independently determine the effect of each of the three variables, multilayered laminar composites of widely varying architectures and compressive layer compositions were fabricated via a sequential slip casting technique described elsewhere [3]. Laminate architectures for each of the three studies were chosen such that two of the three parameters were held nearly constant. Specifics of the laminate architectures (i.e. compressive and tensile layer thickness and compressive layer compositions) used for each study are detailed in the results section.

All laminate specimens contained thicker, tensile layers composed of 0.95 volume fraction $\text{Al}_2\text{O}_3^\dagger$ and 0.05 volume fraction $\text{Zr}(3\text{Y})\text{O}_2^\ddagger$; the ZrO_2 was included for control of grain

[†] AKP-15, $d_{50}=0.6 \mu\text{m}$, Sumitomo, Japan

[‡] TZ-3Ys, $d_{50}=0.4 \mu\text{m}$, Tosoh, Japan

growth. Compressive layers were fabricated from different mixtures of mullite[§] and Al₂O₃. The fraction of mullite was one factor that determined the magnitude of compressive stress. For the thicker, tensile layers containing Al₂O₃ (+ 0.05 volume fraction Zr(3Y)O₂), dispersed aqueous slurries containing 0.30 volume fraction solids were formulated at pH 11 using tetramethyl ammonium hydroxide (TMA-OH). Dispersed, aqueous slurries containing 0.15 volume fraction of the mullite/Al₂O₃ mixture used to form the compressive layers, were formulated at the same pH, homogenized by attrition milling (Union Process Szegvari Attritor, 3 mm Zr(3Y)O₂ milling media), and then allowed to equilibrate for 12 hours prior to casting. The magnitude of residual compression, σ_c , within the compressive layers was varied by changing the volume fraction of mullite within the compressive layers from 0.10 to 0.70 (balance Al₂O₃). Although different laminar architectures were fabricated to investigate the effect of architecture on the threshold strength, architectures were fabricated with similar layer thickness ratios in an attempt to keep the compressive stress nearly identical for the different architectures produced with the same material combinations.

Laminate plates (approximately 70 x 60 x 4 mm before firing) were cast, dried at room temperature for several days, and fired at 1550°C/2 hrs in air (5°C/min heating and cooling rate). (Masa, you need to explain that the periodic compressive layers only existed in the center portion, whereas the outer layer was thick (1000 μm) –you might also show this in a figure. Explain that this reduced the time for specimen fabrication. The reason you need to do this is where the threshold strength is about the same as the mean failure strength of the monolith). Flexural bars were diamond cut (approximately 3.5 x 3 x 50mm) from the plates and one of the lateral surfaces of each specimen was polished to a 6 μm finish with a diamond abrasive. With a Vickers indenter and loads between 2 and 5 kg, cracks of varying size (~100 - 300 μm) were introduced into the center of the central Al₂O₃ layer on the polished surface of each specimen. The indenter cracks ensured that stable crack extension would occur through the compressive layers with increasing applied stress, which would enabled the measurement of a threshold strength.

Monolithic control specimens (without compressive layers) of the tensile layer composition were also fabricated by the same procedure outlined above. Identical indenter cracks were also introduced into the control specimens. In addition, a set of control specimens were produced that did not have indenter cracks.

2.2 *Residual, Compressive Stress Determination*

Biaxial residual compressive stresses produced by the differential thermal contraction of the laminae during cooling from the densification temperature were determined using Eq. (2) and the property data listed in Table 1. In these calculations, it was assumed that all differential strain was dissipated via creep until the materials were cooled to 1200 °C [4].

[§] MULSM, $d_{50}=0.7 \mu\text{m}$, Baikowski, France

Material	α ($\times 10^{-6} \text{ C}^{-1}$)	E (GPa)	ν	K (GPa)
Al_2O_3	8.30 (5)	401 (5)	0.22 (5)	166 (5)
$\text{Zr(3Y)}\text{O}_2$	11.35 (2)	205 (2)	0.32 (2)	N/A
Mullite	5.30 (5)	220 (5)	0.27 (5)	157 (5)

Table 1. Materials property data for laminate constituents. References are included in parenthesis next to values.

The elastic modulus of the multiphase compressive layers was estimated using the lower bound estimate of Ravichandran [6],

$$E = \frac{(cE_1E_2 + E_2^2)(1+c)^2 - E_2^2 + E_1E_2}{(cE_1 + E_2)(1+c)^2} \quad (4)$$

where E_1 and E_2 are the moduli of the two constituent phases, the non dimensional parameter $c = (1/V_1)^{1/3} - 1$, and V_1 is the volume fraction of the minor phase. The coefficient of thermal expansion was estimated using the analysis of Turner [7],

$$\alpha = \frac{\alpha_1 K_1 V_1 + \alpha_2 K_2 V_2}{K_1 V_1 + K_2 V_2} \quad (5)$$

where α_i is the coefficient of thermal expansion of either constituent, K_i the bulk modulus, and V_i the volume fraction. The Poisson's ratio, however, was estimated using a simple rule of mixtures, as suggested by Ravichandran [6]. The rule of mixtures was also used to determine the properties of the multiphase tensile layers as well, due to the small volume fraction of the second phase within the tensile layers.

The residual compressive stresses within the thin compressive layers of some representative architectures were (Masa-you're not verified anything, you are MEASURING. You will then compare the CALCULATED vaues with the MEASURED values!!!! and then make some comment, e.g., the comparision is pore, good, excellent, etc, etc!!!!) measured using a piezospectroscopic method in which uses the stress-induced shift in the fluorescence spectra of trace Cr^{3+} impurities in alumina [8]. Following a procedure described elsewhere [9], fluorescence spectra were taken well away from the free edges, on the polished surface of compressive layers in laminates which had been ground down at a shallow angle ($\sim 1^\circ$) relative to the laminar plane to form a wedge. By examining only the thickest part of the compressive layer, the contribution of the underlying tensile Al_2O_3 layer's fluorescence spectra was minimized, therefore ensuring an accurate stress measurement within the compressive layer.

2.3 Mechanical Testing

All specimens were tested in the transverse 4-point flexure configuration (i.e. loading direction parallel to the laminate plane) [1,10] using a screw-driven mechanical testing machine operating in displacement control mode (Instron Model 8562, crosshead speed = 0.01 mm/min,

spans = 13 and 30 mm), such that the indented face of the specimen was put in tension. The tensile stress applied to the crack on the surface of the specimen, σ_a , was calculated by substituting the applied load and specimen dimensions into the bending beam formula for 4-point flexural loading

$$\sigma_a = \frac{3P_a(s_o - s_i)}{2bh^2} \quad (6)$$

where P_a is the applied load, s_o and s_i the outer and inner spans, b the specimen width, and h the specimen height. Observations of the crack on the tensile surface of the laminate specimens during loading showed that, in all cases, extension and arrest of the indenter crack occurred before failure, therefore indicating that the measured failure strength was the threshold strength.

2.4 Crack Path Observations

As reported below, observations of the fracture surfaces indicated that the crack would either propagate straight across the compressive layer or bifurcate as it entered the compressive layer. Utilizing procedures detailed elsewhere [10], crack extension on the external tensile surface of select specimens was observed during loading with cellulose acetate replicas. As shown below, bifurcation could only be revealed by observing the crack path beneath the surface. To view the crack path beneath the surface, select specimens were loaded to a stress just below their failure strength and then unloaded. The material on the tensile surface was then removed to a depth of ~50 μm from the original surface and the specimen was repolished and observed under an optical microscope (Nikon Eclipse ME600). Fracture surfaces also detailed the path of bifurcating cracks when observed using scanning electron microscopy (JOEL Model 6300).

2 Results

3.1 Effect of the Magnitude of Residual Compression, σ_c

Two different laminate architectures, one composed of 200 μm tensile layers and 25 μm compressive layers (hereafter designated as 200/25), and the other composed of 550 μm tensile layers and 55 μm compressive layers (hereafter designated as 550/55) were produced for this study. It was hoped that the use of this dual architecture strategy would allow probing of the critical thickness condition for one or more of the residual stress states chosen, i.e. for a given compressive layer composition bifurcation would occur in the thicker 550/55 laminate, but not in the thinner 200/25 one.

The threshold strengths measured for the 550/55 and 200/25 laminates are reported in Fig.1 and Table 2, along with the strengths predicted by Eq. (3), assuming a value of $K_c = 2.7 \text{ MPa}\cdot\text{m}^{1/2}$ for the mullite/alumina materials [11]. Figure 1 also reports the strengths of the monolithic specimens, with and without indenter cracks. Table 2 also reports the values of residual compression estimated by Eq. (2), and the values measured for selected 550/55 specimens using piezospectroscopy.

Table 2. Estimated and measured values of residual compression and threshold strength for

Compressive Layer, t_i Composition (v. fract. mullite)	200/25 Laminate				550/55 Laminate			
	Resid. Compr., σ_c		Threshold Str., σ_{thr}		Resid. Compr., σ_c		Threshold Str., σ_{thr}	
	Eq. (2)	meas.	Eq. (3)	meas.	Eq. (2)	meas.	Eq. (3)	meas.
	(MPa)	(MPa)	(MPa)	(MPa)	(MPa)	(MPa)	(MPa)	(MPa)
0.10	192 ±1		202 ±3	191 ±3	194 ±0		144 ±1	151 ±5
0.25	344 ±2		251 ±1	256 ±5	352 ±2	363 ±2	191 ±2	210 ±4
0.40	491 ±2		307 ±2	390 ±11	506 ±1	541 ±2	237 ±1	378 ±10
0.55	646 ±5		349 ±5	531 ±11	657 ±2	736 ±4	283 ±2	462 ±7
0.70	779		409	617	799 ±1	859 ±1	334 ±2	535 ±20

laminates used for the residual compression effect study.

Five specimens were tested for all data points shown in Fig. 1; all but one had standard deviations $\leq 5\%$. The one exception was for the 0.70 volume fraction mullite 200/25 laminate, where only one specimen out of 15 failed from the indenter crack. Lack of failure from the indentation cracks was due to the fact that processing constraints dictated that the series of 25 μm compressive layers that sandwiched the 200 μm alumina layers was itself sandwiched between much thicker layers ($\approx 1000 \mu\text{m}$) of monolithic alumina that composed the other surfaces of the specimens. Because the threshold strength of this specific architecture approached that of the average strength of the alumina itself, failure in all but one specimen initiated from defects within the thick outer alumina layers. Fractography revealed that the indenter cracks had only partially propagated through their bounding compressive layers prior to the catastrophic failure caused by the unrestrained propagation of cracking in the thick outer layers.

As can be seen in Fig. 1, the experimental data closely followed that predicted by Eq. (3) for the laminates in which the magnitude of residual compression is low (0.10 and 0.25 volume fraction mullite). In addition, the fracture surfaces of these laminates were observed to be relatively flat, indicating that the crack propagated straight across the compressive layer, as predicted by the model. Conversely, Fig. 1 also reflects the inability of the model to accurately describe the threshold strength when the level of residual compression is large (0.40, 0.55, and 0.70 volume fraction laminates). For the other cases, where the threshold strength was larger than that predicted by Eq (3), the crack stepped from one layer to another, which as detailed below, was indicative of crack bifurcation.

3.2 Effect of Compressive Layer Thicknesses, t_1

The effect of the compressive layer thickness, t_1 , on the threshold strength was investigated by fabricating compressive layers with thicknesses ranging from ~20 to ~70 μm for two different sets of laminate architectures where the tensile layer thickness was fixed at 500 μm . The two different laminate architectures, one composed of compressive layers formed of 0.25 volume fraction mullite (balance Al_2O_3), and the other composed of compressive layers formed of 0.40 volume fraction mullite (balance Al_2O_3) were chosen in the hopes that they would illustrate the critical residual compression dependence of bifurcation for any and/or all of the given compressive layer thicknesses. The chosen laminate architectures also ensured that the residual compression within the compressive layers of laminates of the same compressive layer composition varied by no more than 10% from one another

500 / xx μm 0.25 vol. Fract. Mulli				500 / xx μm 0.40 vol. Fract. Mullite			
Compressive Layer Thickness, t_1 (μm)	Residual Compr., σ_c , est. by Eq. (2) (MPa)	Threshold Str., σ_{thr}		Compressive Layer Thickness, t_1 (μm)	Residual Compr., σ_c , est. by Eq. (2) (MPa)	Threshold Str., σ_{thr}	
		Eq. (3) (MPa)	meas. (MPa)			Eq. (3) (MPa)	meas. (MPa)
19 \pm 1	369 \pm 1	171 \pm 2	165 \pm 1	23 \pm 1	527 \pm 1	211 \pm 2	237 \pm 7
35 \pm 0	359 \pm 0	188 \pm 1	194 \pm 4	35 \pm 2	516 \pm 1	231 2	294 \pm 13
54 \pm 4	352 \pm 2	191 \pm 2	210 \pm 4	54 \pm 1	506 \pm 1	237 \pm 1	378 \pm 10
74 \pm 1	338 \pm 0	204 \pm 1	234 \pm 6	71 \pm 1	488 \pm 2	257 \pm 2	421 \pm 9

Table 3. Estimated and measured values of threshold strength and estimated values of residual compression for laminates used in the compressive layer thickness effect study.

Table 3 and Fig. 2 report the threshold strength for these laminates, along with the strengths estimated by the application of Eq. (3). The strengths of the indented monoliths are also reported in Fig. 2 for comparison. Five specimens were tested for all data points in Fig. 2 and the standard deviation of each point was $\leq 5\%$.

Figure 2 shows, once again, that the model only accurately describes the behavior of the laminates when either the level of residual compression is low (all 0.25 volume fraction laminates) or the compressive layer thickness is small (0.40 volume fraction mullite laminate with 23 μm compressive layers). As before, the fracture surfaces of the laminates that fell within predictions were flat, whereas those that deviated from the predictions were stepped. It can also be seen that, in the laminates which displayed this stepping, the magnitude of the deviation of the measured threshold strengths from those predicted by Eq. (3) increased with increasing compressive layer thickness.

3.3 Effect of Tensile Layer Thicknesses, t_2

The effect of tensile layer thickness, t_2 , on the threshold strength was investigated by varying the tensile layer thickness from ~ 200 to ~ 500 μm in two different sets of laminate architectures with a compressive layer thickness fixed at 25 μm . Table 4 and Fig. 3 report these measurements along with the estimates of residual stress and threshold strength determined by application of Eqs. (2) and (3), respectively. The strengths of the indented monoliths with two different indentation loads (2 and 5 kg) are presented in Fig. 3 for comparisons. Two different indenter loads were required in this part of the study to ensure that the precrack was large enough to cause cracking to initiate at a stress below the threshold strength, but not so large that it affected the residual stress distribution within the compressive layers [12]. Five specimens were tested for all data points in Fig. 3 and the standard deviation of each point was less than 5%.

xxx / 25 μm 0.25 vol. Fract. Mulli				xxx / 25 μm 0.40 vol. Fract. Mullite			
Tensile Layer Thickness, t_2 (μm)	Residual Compr., σ_c , est. by Eq. (2) (MPa)	Threshold Str., σ_{thr}		Tensile Layer Thickness, t_2 (μm)	Residual Compr., σ_c , est. by Eq. (2) (MPa)	Threshold Str., σ_{thr}	
		est. (MPa)	meas. (MPa)			est. (MPa)	meas. (MPa)
210 \pm 0	344 \pm 2	248 \pm 1	256 \pm 5	188 \pm 4	491 \pm 2	309 \pm 2	390 \pm 11
269 \pm 7	357 \pm 1	222 \pm 1	227 \pm 5	266 \pm 5	511 \pm 1	271 \pm 2	324 \pm 10
353 \pm 4	362 \pm 1	202 \pm 1	213 \pm 2	361 \pm 2	520 \pm 2	239 \pm 2	296 \pm 6
502 \pm 4	369 \pm 1	171 \pm 2	165 \pm 1	508 \pm 4	527 \pm 1	211 \pm 2	237 \pm 7

Table 4. Estimated and measured values of threshold strength and estimated values of residual compression for laminates used in the tensile layer thickness effect study.

Figure 3 shows, as did Figs. 1 and 2 earlier, that the model only accurately describes the behavior of the laminates in which the level of residual compression is low (all 0.25 volume fraction laminates). As before, the fracture surfaces of the laminates that fell within predictions were flat, whereas those that deviated from the predictions were stepped.

3.4 Observations of Crack Paths in Bifurcating Laminates

As reported elsewhere [10] crack replication experiments for laminates where either the compressive stress and/or the thickness of the compressive layer was small showed that the crack extends straight across the compressive layer. Concurrent K determinations for these specimens showed that Eq (1) was in good agreement with the experimental results. In the current study, specimens that exhibit this behavior are those shown in Figs. 1, 2, and 3 which have threshold strengths that agree with those predicted by Eq. 3. These specimens also produced flat fracture surfaces.

Specimens that exhibited crack bifurcation also contained an edge crack that ran along the center of the compressive layer as shown in Fig. 4. As detailed elsewhere, the edge cracks are caused by tensile stresses that arise at and close to the surface where the compressive layer is terminated by a free surface, and they are only produced when the combination of the compressive stress and the thickness of the compressive layer exceeds a critical value. [13].

Edge cracks only extend to a depth that is related to the thickness of the compressive layer. [13] As shown in Fig. 4, the crack that was observed by replication on the free surface propagated straight through the compressive layer until it stopped at the edge crack. Catastrophic failure did not occur when the crack stopped at the edge crack, but at a higher stress, without any apparent extension of the crack on the free surface. As shown in Fig. 5, observations of the fracture surface showed that the straight extension of the crack only occurred near the free surface (within $\approx 30 \mu\text{m}$ for the architecture shown in Fig. 5). For distances from the free surface that were greater than the depth of the edge crack, Fig. 5 shows that the crack propagated across the compressive layer at an angle.

Although close examination of the fracture surfaces did show that cracks that enter the compressive layer do so by bifurcation, a second method for observing the crack path that required removing material from the free surface by diamond grinding, then polishing, best detailed the bifurcation phenomena. Figure 6 clearly shows that the crack bifurcates as it enters the compressive layer. For these observations, the edge crack is also observed, but it is an artifact because it only propagates deeper into the compressive layer as material is removed by diamond grinding. The fact that the edge crack is an artifact of material removal can not only be confirmed by observing fracture surfaces, but as by the observation shown in Fig. 6 itself. Namely, because the edge crack does not exist between the two branches of the bifurcated crack, it confirms the fact that the bifurcated crack existed before the edge propagated deeper into the compressive layer during material removal.

The angles each branch of the bifurcated crack forms with its bisector are 57.5° , 61.0° , and 67.5° for the 0.40, 0.55, and 0.70 volume fraction mullite specimens, respectively. Therefore, given the otherwise similar architectures of these three specimens, the observations indicate that the bifurcation deflection angle increases with the residual compression within the compressive layers.

4 Discussion

It is immediately apparent from Figs. 1-3 that the experimental data for laminates with thin compressive layers and/or low levels of residual compression agree well with that predicted by Eq. (3). For laminates where agreement was good, crack extension occurred straight across the compressive layer which was the crack path used to develop Eq (3). In addition, previous stress intensity factor determinations [10] have shown excellent agreement for these conditions.

On the other hand, Figs. 1-3 also reflect the inability of Eq. (3) to describe the threshold strength when the compressive layer thickness and/or level of residual compression is large; namely, the threshold strength is larger than that predicted. In each of these cases the crack bifurcates as it propagates through the compressive layer. While, quantitative explanation of the cause of bifurcation and its contribution to the threshold strength is beyond the scope of the current work, but it is the subject of current research.

It is interesting to note that while bifurcation is clearly evident in the laminates with thick compressive layers and/or large levels of residual compression, this bifurcation does not share

the same characteristic "mountain-like" fracture surface morphology that has been observed in previous studies [18-20]. where bifurcation occurs during flexural loading. In these studies, the bifurcated crack was observed to propagate down to and then along the midplane of the compressive layer. However, as can be seen in Fig. 6, this type of behavior was not seen in the current study. This discrepancy is likely due to the differences in loading configuration used for each study. Despite the fact that 4-point flexure was used in each of these studies, in the previous studies the loading axis was normal to the laminar plane, while in the current study it was parallel. The stress gradient developed within specimens tested with the loading axis normal to the laminar plane can provide driving force for the propagation of cracking along the laminar plane. No such driving force exists when the loading axis is parallel to the laminar plane, thus perhaps explaining why the crack does not proceed parallel to the tensile axis.

Conclusions

The previously reported model [1] describing threshold strengths in laminar composites is valid only when the crack propagates straight through the compressive layer, as assumed by the model. This only occurs when the compressive stress and/or thickness of the compressive layer is small. At larger compressive stresses and/or compressive layer thicknesses, the crack bifurcates as it propagates through the compressive layer and produces a threshold strength much larger than predicted by the model.

Acknowledgements

The authors would like to thank Vladimir Tolpygo for his assistance in making the piezospectroscopic measurements used to verify the calculated value of the residual stress within the compressive layers. This work was supported by the Office of Naval Research under grant N00014-99-1-0638.

REFERENCES

- [1] M. P. Rao, A. J. Sánchez-Herencia, G. E. Beltz, R. M. McMeeking, and F. F. Lange, "Laminar Ceramics That Exhibit a Threshold Strength," *Science*, **286** 102-105 (1999).
- [2] C. Hillman, Z. Suo, and F. F. Lange, "Cracking of Laminates Subjected to Biaxial Tensile Stresses," *J. Am. Ceram. Soc.*, **79** [8] 2127-33 (1996).
- [3] J. Requena, R. Moreno, and J. S. Moya, "Alumina and Alumina/Zirconia Multilayer Composites by Slip Casting," *J. Am. Ceram. Soc.*, **72** [8] 1511-13 (1989).
- [4] V. Sergo, X. Wang, D. R. Clarke, and P. F. Becher, "Residual Stresses in Alumina/Ceria-Stabilized Zirconia Composites," *J. Am. Ceram. Soc.*, **78** [8] 2213-14 (1995).
- [5] B. R. Marple and D. J. Green, "Mullite/Alumina Particulate Composites by Infiltration Processing: IV, Residual Stress Profiles," *J. Am. Ceram. Soc.*, **75** [1] 44-51 (1992).
- [6] K. Ravichandran, "Elastic Properties of Two Phase Composites," *J. Am. Ceram. Soc.*, **77** [5] 1178-84 (1994).

- [7] P. S. Turner, "Thermal-Expansion Stresses in Reinforced Plastics," *J. Res. Natl. Stand. (U.S.)*, **37**, 239-50 (1946).
- [8] Q. Ma and D. R. Clarke, "Piezospectroscopic Determination of Residual Stresses in Polycrystalline Alumina," *J. Am. Ceram. Soc.* **77** [2] 298-302 (1994).
- [9] V. Sergo, D. M Lipkin, G. De Portu, and D. R. Clarke, "Edge Stresses in Alumina/Zirconia Laminates," *J. Am. Ceram. Soc.* **80** [7] 1633-38 (1997).
- [10] M. P. Rao, J. Rödel, and F. F. Lange, "Residual Stress Induced R-Curves in Laminar Ceramics that Exhibit a Threshold Strength," *submitted to J. Am. Ceram. Soc.*
- [11] A. Khan, H. M. Chan, M. P. Harmer, and R. F. Cook, "Toughness-Curve Behavior of an Alumina-Mullite Composite," *J. Am. Ceram. Soc.*, **81** [10] 2613-23 (1998).
- [12] **indent residual stress field Marshall**
- [13] S. Ho, C. D. Hillman, F. F. Lange, and Z. Suo, "Surface Cracking in Layers Under Biaxial, Residual Compressive Stress," *J. Am. Ceram. Soc.*, **78** [9] 2353-59 (1995).
- [14] M. Y. He, A. G. Evans, and J. W. Hutchinson, "Crack Deflection At An Interface Between Dissimilar Elastic Materials: Role of Residual Stresses," *Int. J. Solids Structures*, **31** [24] 3443-3455 (1994).
- [15] O. Prakash, P. Sarkar, and P. S. Nicholson, "Crack Deflection in Ceramic/Ceramic Laminates with Strong Interfaces," *J. Am. Ceram. Soc.*, **78** [4] 21125-27 (1995).
- [16] J. S. Moya, A.J. Sánchez-Herencia, J. F. Bartolomé, and T. Tanimoto, "Elastic Modulus in Rigid Al₂O₃/ZrO₂ Ceramic Laminates," *Scripta Materialia*, **37** [7] 1095-1103 (1997).
- [17] K. Hbaieb, M. P. Rao, F. F. Lange, and R. M. McMeeking, *work in progress*.
- [18] M. Oechsner, C. Hillman, and F.F. Lange, "Crack Bifurcation in Laminar Ceramic Composites," *J. Am. Ceram. Soc.*, **79** [7] 1834-38 (1995).
- [19] A. J. Sánchez-Herencia, C. Pascual, J. He, and F. F. Lange, " ZrO₂/ZrO₂ Layered Composites for Crack Bifurcation," *J. Am. Ceram. Soc.*, **82** [6] 1512-18 (1999).
- [20] A. J. Sánchez-Herencia, L. James, and F. F. Lange, " Bifurcation in Alumina Plates Produced by a Phase Transformation in Central, Alumina/Zirconia Thin Layers," *J. Eur. Ceram. Soc.*, **20** [9] 1295-1300 (2000).

FIGURES

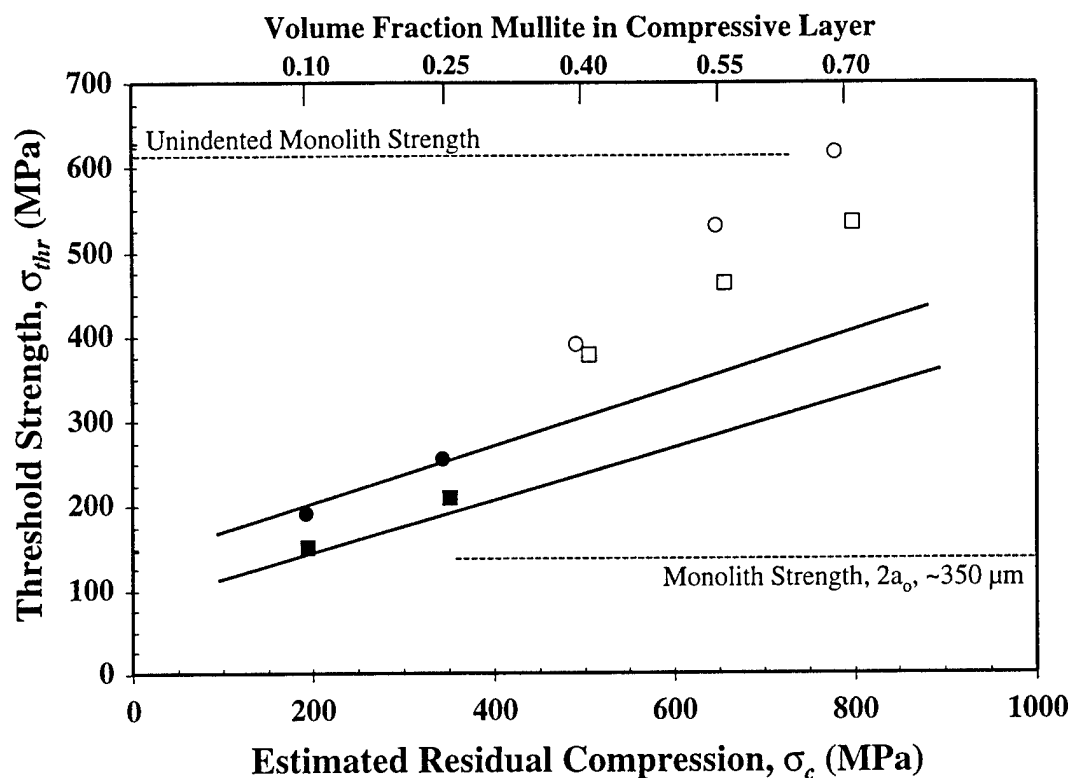


FIG. 1 Plot of measured threshold strength vs. magnitude of residual compression within the compressive layers. Square and circular symbols denote results for 550/55, and 200/25 laminates, respectively. Open symbols represent specimens in which the fracture surfaces were flat, while closed symbols represent those in which stepping of the fracture surface was observed. Solid lines indicate theory (Eq. 3) predictions based on laminate architecture and magnitude of residual compression. The dashed horizontal line indicates the strength of monolithic specimens of the tensile layer composition that were indented with a 5 kg Vickers indent. Standard deviation for all data points, except the 220/25 0.70 volume fraction point, was less than 5%.

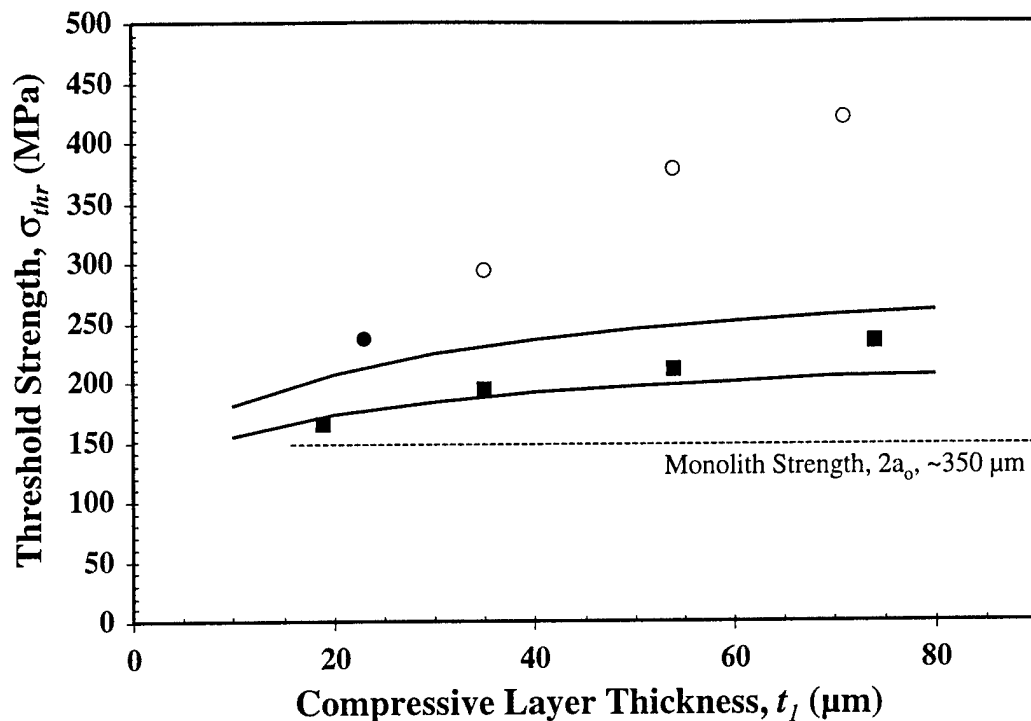


FIG. 2 Plot of measured threshold strength vs. compressive layer thickness. Square and circular symbols denote results for $500 / xx \mu\text{m}$ 0.25 volume fraction mullite and $500 / xx \mu\text{m}$ 0.40 volume fraction mullite specimens, respectively. Open symbols represent specimens in which the fracture surfaces were flat, while closed symbols represent those in which stepping of the fracture surface was observed. Solid lines indicate theory (Eq. 3) predictions based on laminate architecture and magnitude of residual compression. The dashed horizontal line indicates the strength of monolithic specimens of the tensile layer composition that were indented with a 5 kg Vickers indent. Standard deviation for all data points was less than 5%.

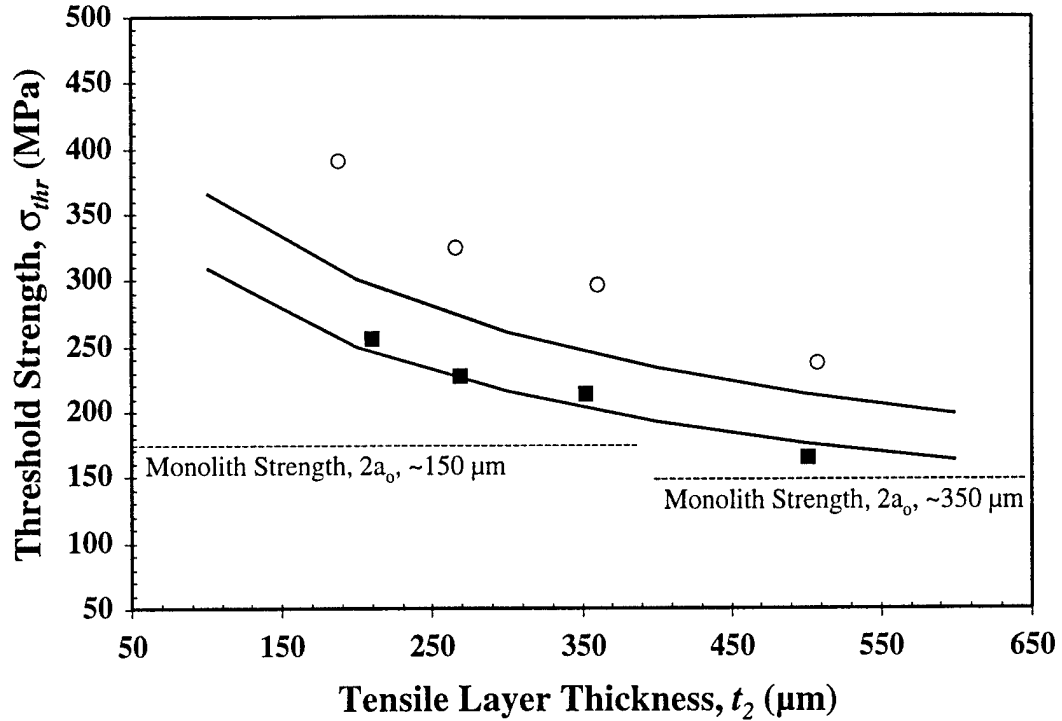


FIG. 3 Plot of measured threshold strength vs. tensile layer thickness. Square and circular symbols denote results for xxx / 25 μm 0.25 volume fraction mullite and xxx / 25 μm 0.40 volume fraction mullite specimens, respectively. Open symbols represent specimens in which the fracture surfaces were flat, while closed symbols represent those in which stepping of the fracture surface was observed. Solid lines indicate theory (Eq. 3) predictions based on laminate architecture and magnitude of residual compression. The dashed horizontal lines indicate the strength of monolithic specimens of the tensile layer composition that were indented with 2 and 5 kg Vickers indents, respectively. Standard deviation for all data points was less than 5%.

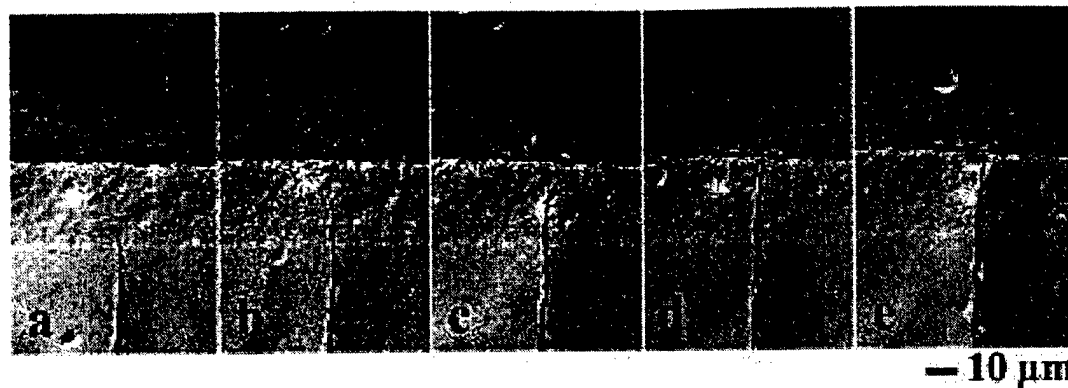


FIG. 4 Optical micrographs of cellulose acetate replicas of the arrested crack within one of the compressive layers of one of the 550/55 0.55 volume fraction mullite specimens taken during loading at applied stresses of: a) 100 MPa; b) 151 MPa; c) 201 MPa; d) 251 MPa; and e) 301 MPa. The specimen withstood further loading to 389 MPa without any further propagation of the crack observed, after which catastrophic failure occurred. Note: Cracking observed along the midplane of the compressive layer occurred before loading and is the edge crack that formed on the new free surface revealed by grinding and polishing.

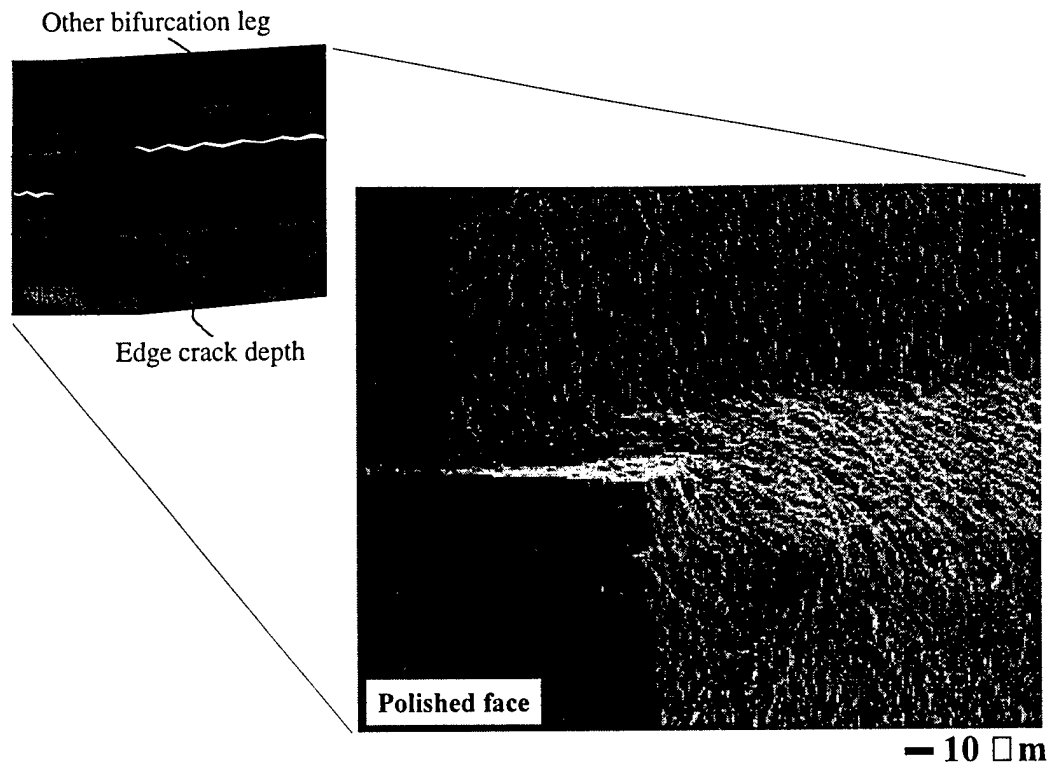


FIG. 5 Schematic and scanning electron micrograph of the fracture surface of one of the 550/55 0.55 volume fraction mullite specimens in the region near the tensile face of the bar (smooth area on left of picture) showing the transition between the cracking observed on the tensile surface (see Fig. 4) and the bifurcation that occurs within the bulk, beneath the penetration depth of the edge crack (see Fig. 6).

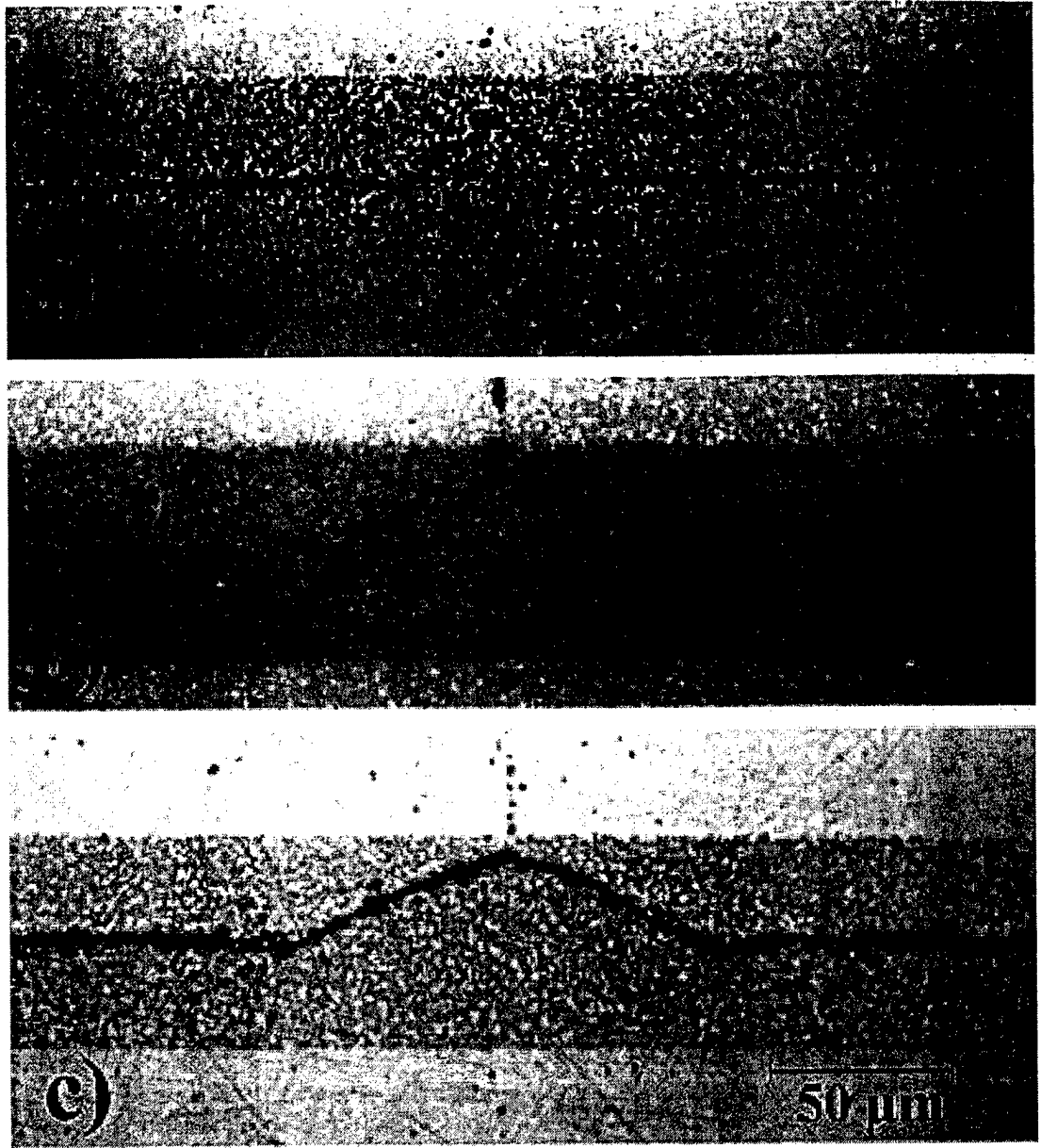


FIG. 5 Optical micrographs of the bifurcation of the crack beneath the tensile surfaces of 550/55 laminates with compressive layer compositions of: a) 0.40 volume fraction mullite; b) 0.55 volume fraction mullite; and c) 0.70 volume fraction mullite. The angles of deflection from the initial crack path measured from the micrographs are 57.5° , 61.0° , and 67.5° , respectively. Note: The observed edge crack reformed on the new free surface exposed by grinding, as is evidenced by its absence between the branches of the bifurcated crack where the tensile surface stresses are relieved.

REPORT DOCUMENTATION PAGE			Form Approved OMB No. 0705-0188	
1. AGENCY USE ONLY (Leave blank)	2. REPORT DATE Feb 10, 2000	3. REPORT TYPE AND DATES COVERED Technical Repts. # 4 5/1/00 through 4/30/01		
4. TITLE AND SUBTITLE Reliable Ceramic Structural Composites Designed with a Threshold Strength			5. FUNDING NUMBERS N00014-99-1-0638	
6. AUTHOR(S) PII: Fred F. Lange				
7. PERFORMING ORGANIZATION NAME(S) AND ADDRESS(ES) Materials Department College of Engineering University of California Santa Barbara, CA 93106-5050			8. PERFORMING ORGANIZATION REPORT NUMBER NA	
9. SPONSORING/MONITORING AGENCY NAME(S) AND ADDRESS(ES)			10. SPONSORING/MONITORING AGENCY REPORT NUMBER	
11. SUPPLEMENTARY NOTES The views, opinions and/or findings contained in this report are those of the author(s) and should not be construed as an official Department of the Army position, policy or decision, unless so designated by other documentation.				
12A. DISTRIBUTION/AVAILABILITY STATEMENT Approved for public release; distribution unlimited.			12B. DISTRIBUTION CODE	
13. ABSTRACT (Maximum 200 words) Compressive layers, placed within a laminate, can arrest cracks. With an increasing applied stress, the arrested crack can propagate through the compressive layer. These phenomena produce a material with a threshold strength, i.e., failure can not occur below a critical stress. A previously reported stress intensity function describes different variables, e.g., magnitude of compressive stress, thickness of compressive layer, distance between compressive layers, that govern the threshold strength. Laminar composites composed of thicker alumina layers separated by thinner alumina/mullite layers were fabricated to test the different variables that were predicted to govern the threshold strength. It is shown that the data agree well with the predicted values only when the magnitude of the compressive stress and/or the thickness of the compressive stress were low. For these conditions, the crack extended straight through the compressive layers as assumed by the model used to predict the threshold strength. On the other hand, when the compressive stress and/or the layer thickness were large the threshold strength was larger than the predicted value. In addition, for these conditions the crack bifurcated through the compressive layer. The angle between the bifurcated cracks increased with increasing compressive stress.				
14. SUBJECT TERMS			15. NUMBER OF PAGES 22 pages	
			16. PRICE CODE	
17. SECURITY CLASSIFICATION OF REPORT Unclassified	18. SECURITY CLASSIFICATION OF THIS PAGE Unclassified	19. SECURITY CLASSIFICATION OF ABSTRACT Unclassified	20. LIMITATION OF ABSTRACT UL	